An Observation of the Sculptures of the Vessel Wall of *Fagus crenata* BL. Using Scanning Electron Microscopy.

By

Jun OHTANI* and Shigeo ISHIDA*

走査型電子顕微鏡によるブナの道管膜の Sculptures の観察

大谷 諄*・石田茂雄*

CONTENTS

Introduction

The general nature of the structure of the wood cell wall is complicated by sculptures, such as pits, perforation plate, warts, spiral thickenings......, arising as normal feature of the wood cell wall[15]. Exact knowledge of the structure of the sculptures, therefore, is of significance for better understanding of the actual cell wall structure. Valuable informations of the fine structure of the sculptures in the hardwoods obtained with electron microscopy have been reported[3,4,5,9,16,17,18].

* Laboratory of Wood Physics, Dept. of Forest Products, Faculty of Agriculture, Hokkaido University.
北海道大学農学部　林産学科　木材理学教室

The fine structure of the sculptures of the wall of vessels in the hardwoods which are very important not only for conducting water in a living tree but also for the physical properties of wood, however, has not received as much study as that of tracheid wall in the softwoods. The findings in the vessel, as well as the other elements, in the hardwood, moreover, have not provided the information for the structural variation within an annual ring.

The scanning electron microscopy is very useful for the study of sculptures, because of a great depth of focus of the microscope, and of the relatively large size of specimen with which the three dimensional structure and its structural variation can be examined.

From the standpoint mentioned above, the writers have studied for these years on the sculptures in the hardwoods using the scanning electron microscopy, and it became evident that the sculptures of vessel wall of *Fagus crenata* BL. were peculiar, especially, in their structural variation within an annual ring. The objective of this paper is to point out some characteristic features in the structure and variation, of warts, pits and perforation plate on the vessel wall of this species.

Methods

The fresh materials were taken at the breast height from living trees of *Fagus crenata* BL. (Diameter B. H.: 50–60 cm) grown in southern Hokkaido. The outer sapwood where no tyloses were found was selected for examining the sculptures of vessel wall for this study. The surfaces to be observed were obtained by splitting, and by cutting using a new razer blade. Specimens were finished in the form of ca. 7 mm × 7 mm × 1 mm and stuck on blass standard stubs for this electron microscope with electric conductive paint. The longitudinal radial surface (7 mm × 7 mm) to be observed was coated with gold. The scanning electron microscope used was model JSM–2 made by Japan Electron Optics Laboratory Co., Ltd. The specimen stage was inclined 45° from the horizontal and 16–25 kV of accelerating voltage was used[10].

Split longitudinal radial surfaces were also examined by the scanning electron microscope after the sodium chlorite-acetic acid treatment[20], in order to observe the microfibrillar orientation of the vessel wall.

Measurement of warts: One annual ring at the outer sapwood was divided radially into five equal parts and they were numbered in turn, I, II, III, IV, V, from earlywood toward latewood. Some normal vessel elements were selected in each part. Measurement for number and size of warts was carried out on the radial wall at the center portion of the vessel elements selected. Warts within an area of 10 μ × 10 μ were counted and the diameter at their bases was measured on the electronmicrographs at the magnification of 20,000 times.

Observation of pits and perforation plate: In order to observe pits and perforation plate from the outer and the inner surfaces of the cell wall of an individual vessel, two kinds of longitudinal radial surfaces, i.e., splitting and cutting, were used in the present study.

Results and Discussion

1. Warts

It is well known that the warty layer is present in tracheids, fibers and vessels in certain hardwoods species[13,14] as well as in tracheids in softwoods. HARADA[8] has reported that wart structure sometimes exists and sometimes does not in a

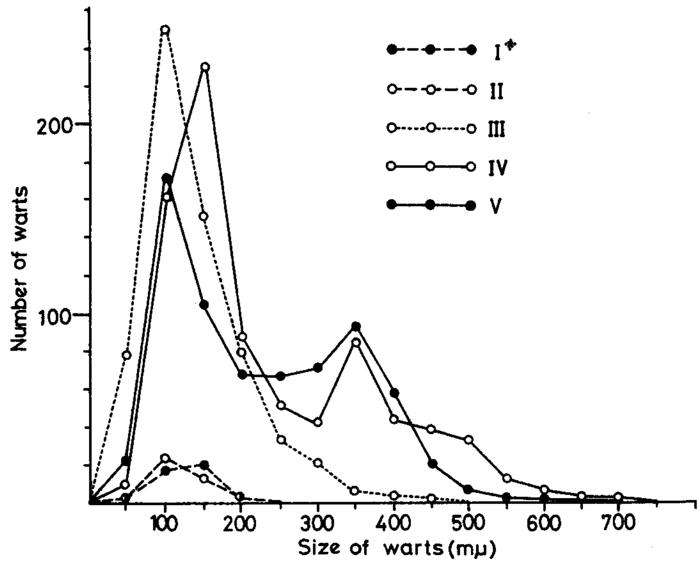

Fig. 1. Size distribution of warts per unit area (100 μ^2) on the vessel wall within an annual ring. Annual ring measured was 0.8 mm in width.

* One annual ring was divided radially into five equal parts and numbered in turn, 「I, II, III, IV, V」, from earlywood to latewood.

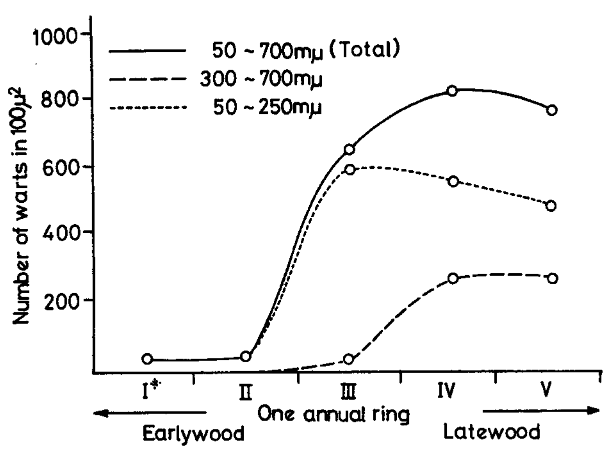

Fig. 2. Variation of warts number per unit area (100 μ^2) on the vessel radial wall within an annual ring.

* See fig. 1.

vessel of *Fagus crenata* BL. The present study on warts of the vessel wall of this species clarified a tendency of variation in number, size and shape of warts, in relation to the position of the vessel within an annual ring: warts are scarcely present in the early stage of an annual increment but remarkably in the late stage.

Figs. 1 and 2 show an example of warts variation in size and number in relation to the position within an annual ring. Warts are scarcely present in the parts I and II as shown in photo 1. Even if present, very small warts, 50–200 mμ in diameter, are scattered irregularly on the wall surface in these parts as in photo 2. These photos also show that the microfibrils of the S_3 layer are oriented almost at a right angle to the vessel axis. In the part III, warts begin to appear more or less clearly. In this part, the inner surface of some vessels was covered with amorphous substances and small particles as shown in photo 3. On the other hand, in some vessels, warts, 50–450 mμ in diameter, were irregular in distribution and appeared as spherical in shape as shown in photos 4 and 5. The most remarkable development of warts was observed in the parts IV and V. Warts congregated and covered uniformly the inner surface of the vessel wall (photos 6 and 7). Diameter of them ranges from 50–700 mμ, and smaller and larger warts coexist as shown in photo 8. In general, well-developed, large warts in these parts are not spherical and are bigger in height than in diameter and they occasionally reach to about 750 mμ in height as shown in photo 9.

The shape and size of warts observed in the present study suggest that warts are not remnants of dead protoplast, but a localized thickening of normal secondary wall. This concept has already been reported from the point of view of warts formation by WARDROP[22] and CRONSHAW[6].

Fig. 3 shows relationship between the radial extent of zone where warts

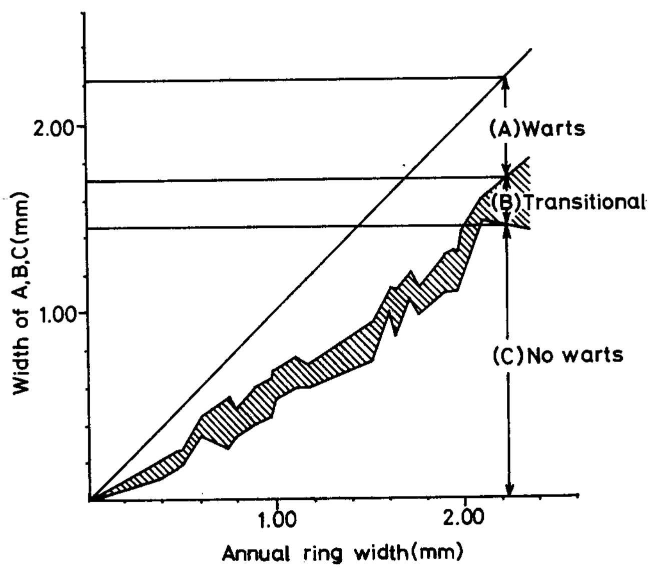

Fig. 3. Relationship between extent of zone where warts distribute within an annual ring and annual ring width.

distribute within an annual ring and the annual ring width. Extent of zone that warts are scarcely present (C in fig. 3) increases with increasing annual ring width, whereas extent of zone that warts are remarkably present (A in fig. 3) increases first slightly and then is held roughly constant with increasing annual ring width. The diameter of vessels in the region where warts are remarkably present is small compared with that in the region where warts are scarcely present. And also it was observed by the optical microscopy that the wood texture of the former is denser than that of the latter. Therefore, it may be quite all right to distinguish roughly between earlywood and latewood based on the degree of warts development.

According to this, earlywood and latewood are defined as parts that warts are scarcely present and remarkably, resp., in this paper by the present authors.

2. Pits

The pits on the wall of a vessel show considerable variations in size, shape and distribution according to the adjacent cell with which the vessel forms the pit pairs. Pits on the vessel wall are, therefore, classified according to the adjacent cells which contact with the vessel as follows;

1. Intervascular pits (V–V pits)
2. Vessel-fiber tracheid pits (V–FT pits)
3. Vessel-tracheid pits (V–T pits)
4. Vessel-ray parenchyma pits (V–R pits)
5. Vessel-longitudinal parenchyma pits (V–P pits)

2-1. Intervascular pits (V–V pits)

Photos 10–17 show V–V pits in the earlywood vessel. It can be seen in photos 11 and 12 that the arrangement of V–V pits is not always typical opposite pitting and the outlines of pits, i.e., the shape of pit annulus, are circular or elliptical in the outer surface view. Pit aperture of V–V pits in the earlywood is slit-like in shape and the direction of its major axis is almost transverse to the vessel axis (photos 10, 11 and 12).

WARDROP[24] has shown a diagrammatic representation of the intervascular pits of hardwoods vessels. According to this, at the pit border the S_1 layer and the S_3 layer are not confluent. And also, it has been demonstrated in the studies on vessel pits in *Fraxinus* by BOSSHARD[2] and in *Ulmus* by WARDROP[21] that initial pit border as seen in softwood tracheids is not recognized in hardwood vessels.

As shown in photos 13, 14 and 15, the S_1 layer does not arch over the pit chamber and the microfibrils of the S_1 layer are circularly arranged near the pit border (labelled S_1 in photo 13). The microfibrils of the S_2 layer surrounding the pit chamber, i.e., on the pit chamber wall, are circularly arranged in some thickness (labelled S_2 in photo 13). In the middle part of the pit border, the microfibrils of the S_2 layer are arranged in the form of two oval half curves and some of them are confluent in the direction of the major axis of pit apertures (photos 14, 15 and 16). Photos 14 and 15 show that the direction of the major axis of the slit-like pit aperture is almost parallel to the main microfibrillar direction of the S_2 layer of the vessel wall (dotted lines in these photos). The microfibrils of the S_3 layer are arranged around the pit aperture on the vessel lumen side (photos 15 and 17). As shown in photos 15 and 17, it was impossible to distinguish exactly between the S_2 layer and the S_3 layer based on the microfibrillar orientation, because of the similarity of the microfibrillar orientation in the two layers.

Photos 18—22 show V–V pits of the latewood vessels. As shown in photos 18 and 19, pit apertures are slit-like or elliptical in shape. The major axis of slit-like aperture is almost transverse to the vessel axis as in the earlywood, whereas the inclination of the major axis of the elliptical aperture is less than that of slit-like and its direction is almost parallel to the microfibrillar orientation of the S_2 layer as shown in photo 20. In the latewood pits, warts pass deep within the pit aperture (photos 18, 19 and 20). This is also shown in photos 21 and 22 in which the development of warts on the pit chamber wall is the most remarkable at the edge of pit aperture and warts decrease gradually from pit aperture to pit annulus. In photo 21, V–V pit of the latewood as seen from the outer surface wall appears as a so-called vestured pit. Such appearances were also found in V–FT pits and V–Rp pits, in the latewood.

It is impossible to decide whether such surface protuberances are so-called vestures or warts based on their shape and size. In this connection, SCHMID[16] has reported that the vestures are formed by the living cytoplasm, whereas the warts are remnants of the dead protoplast, and also that the substances for the vestures are apparently derived from the Golgi vesicles. As stated previously, however, warts are considered as outgrowth of the secondary wall. CRONSHAW[6] has reported that the condensation of the warts material takes place outside the plasma membrane and two possible cytoplasmic systems which could contribute to precursors and enzymes for warts formation are dictyosomes, with the dictyosome derived vesicles, and the endoplasmic reticulum. Therefore, it may be preferable to consider that the origin of both warts and vestures is very resemble.

2-2. Vessel-fiber tracheid pits (V–FT pits)

Photos 23–26 show the V–FT pits of the earlywood vessels. In general, the arrangement of V–FT pits is parallel to vessel axis (photo 23). The outlines of pits are circular in the outer surface view (photos 25 and 26). It was often observed that cytoplasmic residue remained at the pit aperture, especially, in this type of pits (labelled CR in photo 26). Photos 27–29 show the V–FT pits of the latewood vessels. Warts development on the pit chamber wall is the most remarkable at the edge of the pit aperture as in the V–V pits of the latewood (photo 28). Pit apertures of V–FT pits both in earlywood and latewood are slit-like and the major axes of them incline less from the vessel axis than those of V–V pits apertures. The inclination in the earlywood is generally larger than in the latewood (compare photos 24 and 27). It can be seen in photo 29 that the direction of the major axis of pit aperture is almost parallel to the microfibrillar orientation of the S_2 layer. Photo 30 shows the pit membrane of V–FT pit after the sodium chlorite-acetic acid treatment. The microfibrils dispersed randomly could be found, althrough partly, in the pit membrane in this photo.

2-3. Vessel-tracheid pits (V-T pits)

Vessel-tracheid pits are quite similar to V-FT pits in size and shape; therefore, no description is given here about V-T pits.

2-4. Vessel-ray parenchyma pits (V-R pits)

Both procumbent and upright ray cells exist in ray of *Fagus crenata* BL. In photo 31, smaller pits on the surface wall of vessel (at the middle in this photo) are vessel-procumbent ray cell pits (V-Rp pits) and larger ones (at the upper) are vessel-upright ray cell pits (V-Ru pits). Photos 31-34 and 35-37 show V-Rp pits in the earlywood and in the latewood, resp. V-Rp pits are irregular in their distribution on the vessel wall (photos 32 and 33). As shown in photos 33 and 38, it was often observed that no pit pairs were there on the vessel wall which contacted with procumbent ray cells. The outlines of V-Rp pits are circular in the outer surface view (photos 34 and 36). The pit aperture of this type of pits is slit-like or elliptical in shape (photos 32, 35 and 37), and the extended aperture can be apparently observed in the latewood (photos 36 and 37). It can be seen in photo 37 that the direction of the major axis of the pit aperture is almost parallel to the microfibrillar orientation in the S_2 layer as well as in the V-V pits and V-FT pits.

Photos 39-42 show V-Ru pits on the inner surface wall of vessel element. The pit aperture of these is very variable in size and shape (photos 39-42). In general, the aperture of these pits is elliptical in shape and the major axis of the pit aperture is almost transverse to the vessel axis. The circular depressions (arrowed) in the membrane in photos 40 and 41 are considered to be the shape of the pit annulus of the adjoining upright ray cell in the opposite side. In many cases, pit annulus of those upright ray cells forming pit pair seems to be smaller than that of vessel wall. Photo 41 shows unilaterally compound pittings. As shown in photos 39, 40 and 41, pit border of V-Ru pits on the vessel wall is so narrow that the V-Ru pits appear to be simple pits. It can be seen in photo 42 that a thin membrane covers continuously the inner surface of vessel wall and pit membrane. Such a thin membrane has already been found in the inner surface wall of an earlywood vessel in *Robinia*[11]. This thin membrane should be further studied in connection with the warty layer.

2-5. Vessel-longitudinal parenchyma pits (V-P pits)

Photos 43-45 and 46-48 show V-P pits on the vessel wall in the earlywood and the latewood, resp. V-P pits are longitudinally arranged in a row as shown in photos 43 and 46. The size of pit aperture of V-P pits on the inner surface wall of vessel is extremely large compared with that of V-V, V-FT and V-Rp pits. It is easy, therefore, to distinguish V-P pits from the other type of pits due to their size, shape and distribution. Pit apertures on the inner surface wall in the earlywood are elliptical in shape. The major axis of them is almost transverse to vessel axis (photo 43), whereas axis inclination of them in the latewood is less than that in the earlywood (photo 46). It can be seen in photos 47 and 48 that pit aperture is extended, especially in the latewood. The width of pit border in the earlywood is generally narrower than in the latewood as shown in photos 45 and 48.

2-6. The microfibrillar orientation of the secondary wall layers accociated with the pits.

BAILEY and VESTAL[1] investigated the orientation of cellulose in the secondary wall of vessels by the optical microscopy and have concluded that the less specialized types of dicotyledonous vessels resemble normal tracheids in having a 3-layered secondary wall, whereas the more highly specialized types have walls of a much wider range of complexity and structural variability, owing to fluctuations in the orientation of the cellulose. It has been demonstrated in the electron microscopic study of vessel wall in *Fagus* by HARADA[8] and in *Eugenia* by WARDROP[23] that the secondary wall of vessels in these species is distinguished into the typical three layers, viz., outer layer (S_1), middle layer (S_2) and inner layer (S_3). YAMANAKA and HARADA[25] have reported that the organization of the secondary wall in vessels of some species in *Dipterocarpaceae* is different from that developed S_1, S_2 and S_3 layers. So, these evidences show that the layer structure of vessel wall is considerably variable between species.

The typical three layers (S_1, S_2 and S_3) were observed in the vessel wall of *Fagus* in the present study. Photos 49–55 show the microfibrillar orientation of secondary wall. The microfibrils in the S_1 and S_3 layers are oriented almost at a right angle to the vessel axis as shown in photos 49 and 50. The inner surface wall of the S_3 layer in the latewood is covered with the warty layer. The microfibrils in the S_2 layer are oriented at an angle of ca. 30°–50° to the vessel axis and show a Z herical pattern (photos 49–52, 54 and 55). The microfibrillar inclination in the S_2 layer in the latewood is generally less than in the earlywood (compare photos 49 and 54, and photos 51 and 52). As in the tracheid wall of softwood[7], several lamellae of intermediate orientation between the S_1 and the S_2 layers (photo 53), as well as between the S_2 and S_3 layers (photos 54 and 55) were also observed. In photos 53, 54 and 55, it can be seen that the angle of the microfibrillar orientation in these lamellae changes gradually from one to another.

WARDROP[23] has described that the general organization of the secondary wall is greatly disturbed by extensive pitting both on the radial and tangential surfaces of the vessels. On the vessel wall of *Fagus*, microfibrillar orientation of the portion that intervascular pits are crowded is considered to be extremely different from the general pattern in the secondary wall. In this region, except a part of each pit border where microfibrils are circularly oriented, the microfibrils of the S_1, S_2 and S_3 layers follow a sinuous course between adjacent pits and their direction is almost transverse to the vessel axis as a whole (dotted lines in photos 14 and 15).

According to measurement of the vessel wall in *Fagus* by HARADA[8], the proportional thickness of the $P+S_1$, the S_2 and the S_3 to the whole wall is respectively 25%, 50%, and 25%, the S_2 being the thickest. So the microfibrillar orientation of the S_2 layer is the most important to understand the various properties of vessel wall. It was observed in the present study that the direction of the major axis of slit-like and elliptical shaped pit aperture of V–V, V–FT, V–T and V–Rp pits, except V–Ru and V–P pits, was almost parallel to the microfibrillar orientation of the S_2 layer near the each pit. This indicates that the microfibrillar orientation of the S_2 layer within a vessel element can be readily detected by the observaion of the major direction of each pit aperture.

3. Perforation plate

It has been indicated by the optical microscopy that simple perforation and scalariform perforation plate occur between vessel elements of the secondary xylem of *Fagus crenata* BL[19]. But, it is difficult to observe under this means the fine and the three dimensional structures of perforation plate. The present study by the scanning electron microscopy indicated that various types of perforation plates occured in vessels within an annual ring of the species.

Photos 56–60 show the simple perforations of vessels in the earlywood. Photos 56 and 57 show a part of the simple perforation of a vessel in the earlywood. The rims of these simple perforations are situated almost at a right angle to the vessel axis and are not bordered. Photos 57 and 58 show that the rim consists of double cell wall of the adjacent vessel elements. Near the rim of simple perforation, microfibrillar orientation of the S_3 layer is disturbed as shown in these photos. Photos 59 and 60 show a part of simple perforation situating obliquely to vessel axis. The rims of them are bordered. The rims of simple perforations vary in height from the surface of vessel wall (labelled H in photo 56), in degree of bordered and in inclination from the vessel axis. There is a high correlation between the shape of rim and the inclination: simple perforation with lower and non-bordered rim is almost transverse to vessel axis, but one with higher and bordered rim is oblique.

Photos 61–64 show the perforation plates in the early stage of the latewood. Photos 61 and 62 show perforation plate with a bar bridging from a part to the other of the perforation rim. It can be seen in these photos that simple perforation (no bars) occurs in the vessel element in this side (T in photos 61 and 62) and the bar of the opposite side is seen here (O in photos 61 and 62). In photos 63 and 64, most part of many bars are consisted of the cell wall of the vessel element in the opposite side. Photo 64 also shows that these bars in the opposite side are bordered. Some of bars of the vessel element in this side can be found only near the rim (arrowed in photos 63 and 64), but they disappear gradually from the margin toward the center of perforation plate. Photo 65 shows a part of perforation plate with irregularly forked bars. Since such perforation plates were rarely observed, they can be considered as an abnormal.

Various types of multiple perforation plates were observed in the latewood vessels. These are shown in photos 66–80 which show the wide variety of the structure of them. Photos 66 and 67 show a part of scalariform perforation plate, one of the multiple perforation plate. Bars are bordered (photo 67) and the microfibrillar orientation of the S_2 layer in the bars is almost parallel to the axis of bar (arrowed in Photo 67). In the latewood, the inner surface wall of bars are covered with warty layer as shown in photo 68. Such scalariform perforation plates as shown in photos 66 and 67 were rather rare to be observed. Typical scalariform perforation plates with many bars, situating at regular intervals and at a right angle to the vessel axis, were scarcely found in this study. Bars of scalariform perforation plate of *Fagus* are often forked and are not always oriented at a right angle to vessel axis. Photos 69–71 show a part of complex multiple perforation plate with many irregularly forked bars. The inner surface wall of these perforation plates, both in this side and the opposite side, is covered with the warty layer (photos 69 and 70), but the lateral side of bars is not (photo 71). In the photo 71, perforation plate of both vessel elements in this side and the opposite side forms a regular pair, but not in the photos 69 and 70. These perforation plates shown in the both plotos may be merely regarded as reticulate, when they are observed under the optical microscope. As shown in these photos, in many cases, two multiple perforation plates of adjacent vessel elements do not form a regular pair. Typical examples are shown in photos 72–75. In photos 72 and 73, some bars in this side are forked irregularly and the inner surface wall of them is covered with warty layer. Foraminate perforation plate, one of the multiple perforation plate, of vessel element in the opposite side can be seen through the large openings among irregular bars in this side. Photos 74 and 75 show the combination of a typical scalariform perforation plate (in this side) and a foraminate perforation plate (in the opposite side). The structure of each pore in this foraminate perforation plate is considerably similar to that of the intervascular pits apert from lack of closing membrane: they are bordered and pore apertures are slit-like or elliptical in shape. The development of warts on the outer surface wall of pores is the most remarkable at the edge of apertures (arrowed in photo 75). Closing membranes are, however, not found in each pore except in the margin of the perforation plate.

It was also often observed that the membranes remained in the pores located in the margin of the multiple perforation plates mentioned above as shown in photos 76 and 77. Such membranes are made of ramdomly dispersed microfibrils like as primary wall texture.

Photos 78, 79 and 80 show the foraminate perforation plates of the vessels located near the end of annual ring. As these foraminate perforation plates are often inclined slightly from vessel axis, it is difficult to distinguish the perforation plate from the lateral wall of vessel wall. However, perforation plate can be judged by the concentration of pits-like pores and the absence of closing membranes in each pore as shown in photos 79 and 80.

Tracheary elements were also observed in earlywood as shown in photo 81. It is easy to distinguish the tracheary elements from the other cells due to their diameter and cell wall sculptures. They are thin-walled and have many pits on the wall. JAYME and AZZOLA[12] have observed tracheary elements in *Fagus sylvatica* L. which correspond well to the elements observed in this study and they have proposed that such an element should be termed a vascular tracheid. Photo 82 shows the scalariform perforation plate of a tracheary element observed in this study. Bars are bordered and membranes remain at the lateral margin of perforation plate (arrowed photos 82 and 83). Photo 84 shows a pit at the one end of a scalariform perforation plate. This pit membrane is a net-like structure consisting of bundles of microfibrils. This suggests that the structure is a transitional type between pits and pores of perforation plate.

Conclusion

1. Warts on the vessel wall are scarcely present in the early stage and remarkably in the late stage within an annual increment of beech wood studied. It seems to be reasonable, therefore, that the earlywood and latewood of this species are defined based on the degree of warts development.

2. Pits on a vessel wall are classified, according to the kind of adjacent cells which contact with the vessel, as follows; intervascular pits, vessel-fiber tracheid pits, vessel-tracheid pits, vessel-ray parenchyma pits (vessel-procumbent ray cell pits and vessel-upright ray cell pits) and vessel-longitudinal parenchyma pits. Pits on the vessel wall are variable in shape, size and distribution, according to the types of them stated above, and their morphology are also different between the earlywood and the latewood.

Pit aperture of V–V pits and V–Rp pits is slit-like or elliptical in shape. The aperture of V–FT pits and V–T pits is slit-like, while that of V–Ru pits and V–P pits is elliptical. The direction of major axis of slit-like and elliptical pit apertures is almost parallel to the microfibrillar orientation of S_2 layer of the vessel wall in V–V, V–FT, V–T and V–Rp pits, but not clearly related to that in V–Ru and V–P pits.

3. The basic microfibrillar orientation of the S_2 layer in the vessel wall ranges between 30° and 50° from the longitudinal axis of the vessel. However, it is extremely disturbed at the V–V pits region; microscopically, in the pit border of V–V pits, the microfibrils of the S_2 layer on the pit chamber wall i.e., facing to the pit chamber are circularly arranged, whereas those in the middle part of the pit border curve about the pit chamber and are arranged in the form of two oval half curves. Some of them are confluent in the direction of the major axis of the pits aperture. The major axis of pit aperture in the case of slit-like of the V–V pits is almost transverse to the vessel axis, and they are crowded on the vessel, so microfibrils follow a sinuous course between adjacent pits and their direction is, macroscopically, almost transverse to the vessel axis as a whole.

4. Various types of perforation plates were found in an annual ring of the wood studied. Their morphology are closely related to the position within an annual ring, where the vessel locates, thus corresponding to diameter of the vessel

element. Simple perforations occur in large vessel elements, i.e., in the earlywood, on the other hand, multiple perforation plates occur in smaller ones, in the latewood. "Transitional type" between both simple perforation and multiple perforation plate was also found in the transitional zone from the earlywood to the latewood, and in the early latewood. Simple perforation with a rim which has no border and is lower in height is situated almost transversely to the vessel axis, but one with bordered, higher rim is oblique. The angle of inclination from the vessel axis of the multiple perforation plate is generally less than that of the simple perforation.

Multiple perforation plates observed in this study are roughly classified into three types, i.e., scalariform and foraminate perforation plates and perforation plate with bars forked irregularly. It was often found that two different types of multiple perforation plate in the axially adjacent vessel elements contacted with each other, formed an irregular pair.

5. Results obtained in this study on the sculptures provide not only the fundamental information for better understanding of the structure and properties of the vessel itself, but also of the structural variation within an annual ring of beech wood which may help to elucidate the physiological behaviour of the vessel in relation to seasonal wood formation.

Literatures cited

1) BAILEY, I. W., and VESTAL, M. R.: "The orientation of cellulose in the secondary wall of tracheary cells." J. Arnold Arboretum, **18**, 185–195 (1937).

2) BOSSHARD, H. H.: "Elektronenmikroskopische Untersuchungen im Holz von *Fraxinus excelsior* L." Ber. Schweiz. Bot. Ges., **62**, 482–508 (1952).

3) BUTTERFIELD, B. G., and MEYLAN, B. A.: "Perforation plates: observations using scanning electron microscopy." N. Z. J. For. Sci. **1-1**, 116–124 (1971),

4) CÔTÉ, W. A., Jr., and DAY, A. C.: "Vestured pits-Fine structure and apparent relationship with warts." Tappi, **45**, 906–910 (1962).

5) CRONSHAW, J.: "The fine structure of the pits of *Eucalyptus regnans* (F. MUELL.) and their relation to the movement of liquids into the wood." Aust. J. Bot., **8**, 51–57 (1960).

6) CRONSHAW, J.: "The formation of the warts structure in tracheids of *Pinus radiata*." Protoplasma, **2**, 233–242 (1965).

7) HARADA, H., MIYAZAKI, Y., and WAKASHIMA, T.: "Electronmicroscopic investigation on the cell wall structure of wood.". Bull. For. Exp. Sta. Meguro, **104**, 1–115 (1958).

8) HARADA, H.: "Electron microscopy of ultrathin section of beech wood (*Fagus crenata* BL.)." J. Japan Wood Res. Soc., **8**, 252–258 (1962).

9) HARADA, H.: "Ultrastructure of angiosperm vessels and ray parenchyma." in "Cellular ultrastructure of woody plants." CÔTÉ, W. A., Jr., ed., Syracuse Univ. Press, N. Y. 235–249 (1965).

10) ISHIDA, S., and OHTANI, J.: "Study of tyloses by scanning electron microscopy, Report 1. Some preliminary observations of tyloses, mainly in Haru-nire (*Ulmus* sp.)" Res. Bull. College Exp. For. Hokkaido Univ., **26-1**, 1–9 (1968).

11) ISHIDA, S., and OHTANI, J.: "Study on the pit of wood cells using scanning electron microscopy, Report 1. An observation of the vestured pit in black locust, *Robinia pseudoacacia*

Linn." Res. Bull. College Exp. For. Hokkaido Univ., **27-2**, 347-354 (1970).
12) JAYME, G., and AZZOLA, F. K.: "Zur Morphologie der Tracheiden im Rotbuchenholz (*Fagus sylvatica* L.)" Holzforsch., **18**, 9-14 (1964).
13) LIESE, W.: "Zur Struktur der Tertiärwand bei den Laubhölzern." Naturwiss., **44**, 240-241 (1957).
14) LIESE, W.: "The warty layer." in "Cellular ultrastructure of woody plants." CÔTÉ, W. A., Jr., ed., Syracuse Univ. Press, N. Y., 251-269 (1965).
15) PANSHIN, A. J., and de ZEEUW, C.: "Textbook of wood technology.", Third Ed., McGraw-Hill Book Co. (1970).
16) SCHMID, R.: "The fine structure of pits in hardwoods." in "Cellular ultrastructure of woody plants." CÔTÉ, W. A., Jr., ed., Syracuse Univ. Press, N. Y., 291-304 (1965).
17) SCURFIELD, G., and SILVA, S. R.: "The vestured pits of *Eucalyptus regnans* F. MUELL.: a study using scanning electron microscopy," Bot. J. Linn. Soc., **63**, 313-320 (1970).
18) SCURFIELD, G., SILVA, S. R., and INGEL, H. D.: "Vessel wall structure: an investigation using scanning electron microscopy." Aust. J. Bot., **18**, 301-312 (1970).
19) SHIMAJI, K.: "Anatomical studied on the wood of some *Fagus* species" Bull. Tokyo Univ. For., **42**, 181-193 (1952)
20) THOMAS, R. J.: "The development and ultrastructure of the borbered pit membrane." Holzforsch., **22**, 38-43 (1968).
21) WARDROP, A. B.: "The mechanism of surface growth involved in the differentiation of fibers and tracheids." Aust. J. Bot. **2**, 165-174 (1954).
22) WARDROP, A. B., and DAVIES, G. W.: "Warts structure of gymnosperm tracheids." Nature, **194**, 497-498 (1962).
23) WARDROP, A. B.: "Morphological factors involved in the pulping and beating of wood fibers." Svensk Papperstid. **66**, 231-247 (1963).
24) WARDROP, A. B.: "The structure and formation of cell wall in xylem." in "The formation of wood in forest trees." ZIMMERMAM, M., ed., Academic Press, N. Y., 87-134 (1964).
25) YAMANAKA, K., and HARADA, H.: "The ultrastructure of vessel wall in certain species of *Dipterocarpaceae* wood." Bull. Kyoto Univ. For., **20**, 293-300 (1968).

要　約

ブナ (*Fagus crenata* BL.) の道管膜の Sculptures (いぼ状突起，膜孔，せん孔板) の構造及びそれらの年輪内形態変動が走査型電子顕微鏡により観察された。観察の結果，次のように総括・結論する。

1. 年輪内のいぼ状突起のあらわれかたは，特異な傾向がある。即ち，いぼ状突起は年輪内の初期に形成された道管には殆んど存在しないが，後期に形成された道管には顕著に発達している。いぼ状突起の発達の程度をもとにして，早材と晩材を区別することは，他の材構造との関係においても妥当であると考えられる。したがって，本報告では，いぼ状突起が殆んど存在しない部分を早材，いぼ状突起が顕著に発達している部分を晩材とそれぞれ定義し，それらの用語を用いた。

2. 道管膜に存在する膜孔は，道管に接する細胞との間にある膜孔対をもとにして，道管

相互膜孔，道管—繊維状仮道管間膜孔，道管—仮道管間膜孔，道管—放射柔細胞間膜孔（道管—平伏細胞間膜孔，道管—直立細胞間膜孔），道管—軸方向柔細胞間膜孔の種類に分類することができる。道管膜の膜孔は，上記の種類により，それらの形，大きさ，分布などが著しく異なる。又，同一種類の膜孔の形態は，早材・晩材間でも異なる。

道管相互膜孔，道管—平伏細胞間膜孔の膜孔口の形はストット状あるいは楕円であり，道管—繊維状仮道管間膜孔，道管—仮道管間膜孔の膜孔口はスリット状であり，道管—直立細胞間膜孔，道管—軸方向柔細胞間膜孔の膜孔口は楕円である。道管相互膜孔，道管—繊維状仮道管間膜孔，道管—仮道管間膜孔，道管—平伏細胞間膜孔の膜孔口の長軸の方向は，それらの膜孔の付近の二次膜中層のミクロフィブリルの配向とほぼ一致している。

3. 道管膜の二次膜中層のミクロフィブリルは，道管相互膜孔の存在する部分で特異な配向を示す。即ち

[微視的ミクロフィブリルの配向] ミクロフィブリルは，膜孔室と面している付近では円状配向を示し，膜孔縁のその内方では膜孔室を囲むように迂回し，曲がりながら膜孔口の長軸の方向にほぼ平行に配向している。

[巨視的ミクロフィブリルの配向] ミクロフィブリルは，道管軸に対してほぼ直角に，微視的には曲がりくねった波状の配向を示す。このことは，道管相互膜孔が道管膜に密集して存在し，スリット状の膜孔口の長軸の方向が道管軸に対してほぼ直角であることと密接な関連性がある。

4. いろいろな種類のせん孔板が一年輪内に観察された。せん孔板の形態は，せん孔板が存在する道管要素の年輪内の位置と直径に密接な関連がある。即ち，直径の大きな早材道管には単せん孔が存在し，直径の小さな晩材道管には多孔せん孔板が存在する。早材から晩材への移行部，あるいは晩材の初期の部分の道管には，単せん孔と多孔せん孔板の中間型と考えられる特異な形態のせん孔板が存在する。高さの低い有縁でないせん孔縁を有する単せん孔は，高い有縁であるせん孔縁を有する単せん孔より，道管軸に対して大きく傾斜している。多孔せん孔板は，単せん孔より道管軸に対して急傾斜に位置している。

本研究で観察された多孔せん孔板は，階段せん孔板，不規則に枝分れしたバーを有するせん孔板，ほぼ同じ大きさの小孔が群をなしているせん孔板などに大別することができる。これらの多孔せん孔板は，同じ形態のものが整然とした対をなさない場合が多い。

5. Sculptures の構造及びそれらの年輪内形態変動について得られたこれらの結果は，道管の構造や性質のみならず，年輪構造を理解するための基礎的資料を提供するものと考えられる。

Explanation of photographs

Note: The vessel axis in all photographs is vertical. (↕)
All the photographs are of vessel element.

Photo 1. The S_3 layer of a vessel wall in the early stage of an annual increment as seen from the lumen side. Warts are scarcely present. The arrow indicates the direction of the major axis of the vessel.

Photo 2. The S_3 layer of a vessel wall in the early stage of an annual increment as seen from the lumen side. Small warts (arrowed) are scattered irregularly.

Photo 3. Amorphous substances and small particles on a vessel wall of transitional zone from early stage to late stage of an annual increment as seen from the lumen side.

Photo 4. Warts on a vessel wall of transitional zone from early stage to late stage of an annual increment as seen from the lumen side. Spherical warts are irregular in their distribution.

Photo 5. Do. Warts are irregular in their distribution.

Photo 6. Warty layer inside a vessel in the late stage of an annual increment.

Photo 7. Do. Warts cover uniformly the inner surface wall.

Photo 8. A part of photo 7. Small and large warts, two groups in diameter, coexist on the inner surface wall.

Photo 9. Warty layer on the perforation plate in the late stage of an annual increment (cf. photo 68). Well-developed warts reach to 750 $m\mu$ in height as shown in this photo.

Photo 10. V–V pits of an earlywood as seen from the lumen side.

Photo 11. V–V pits of an earlywood vessel. The photo shows V–V pits on the inner surface wall at the right and on the outer surface wall of the opposite vessel element at the left.

Photo 12. V–V pits of an earlywood vessel as seen from the outer surface wall.

Photo 13. An earlywood vessel wall showing the microfibrillar orientation in the V–V pits region. Pit membrane and the S_1 layer of the vessel wall in this side are shown at the left in this photo, the S_1 and the S_2 layers in the opposite side are shown at the right. S_1: outer layer of secondary wall, S_2: middle layer of secondary wall.

Photo 14. An earlywood vessel wall after the sodium chlorite-acetic acid treatment showing the microfibrillar orientation in the V–V pits region. The S_1 layer of the vessel wall in this side and the S_2 layer in the opposite side are shown at the upper (labelled S_1) and at the lower right (labelled S_2), resp. S_1: outer layer of secondary wall, S_2: middle layer of secondary wall, dotted line: the main microfibrillar direction of the S_2 layer.

Photo 15. Do. S_1: outer layer of secondary wall, S_2: middle layer of secondary wall, S_3: inner layer of secondary wall, dotted line: the main microfibrillar direction of the S_2 layer.

Photo 16. V–V pits of an earlywood vessel as seen from the outer surface wall. S_2:

middle layer of secondary wall.

Photo 17. An earlywood vessel wall showing the microfibrillar orientation in the V–V pits region. S_3: inner layer of secondary wall.

Photo 18. V–V pits of a latewood vessel as seen from the lumen side. Pit apertures are slit-like in shape.

Photo 19. Do. Pit apertures are elliptical in shape.

Photo 20. V–V pits of a latewood vessel. The microfibrils (arrowed) in the pit border are circularly oriented. S_2: middle layer of secondary wall.

Photo 21. V–V pit of a latewood vessel as seen from the outer surface wall. The development of warts on the pit chamber wall is the most remarkable at the edge of pit aperture.

Photo 22. V–V pits of a latewood vessel as seen from the outer surface wall.

Photo 23. V–FT pits of an earlywood vessel as seen from the lumen side.

Photo 24. A part of photo 23.

Photo 25. V–FT pits of an earlywood vessel as seen from the outer surface wall.

Photo 26. V–FT pits of an earlywood vessel as seen from the outer surface wall. The cytoplasmic residue (labelled CR) remains at the pit aperture. CR: cytoplasmic residue.

Photo 27. V–FT pit of a latewood vessel as seen from the lumen side. Compare with photo 24.

Photo 28. V–FT pits of a latewood vessel as seen from the outer surface wall.

Photo 29. A latewood vessel wall after the sodium chlorite-acetic acid treatment. The direction of the major axis of pit apertures of V–FT pits is almost parallel to the microfibrillar orientation of the S_2 layer. Arrows show several lamellae of the S_2 layer which indicate similar microfibrillar orientation in each other. S_2: middle layer of secondary wall.

Photo 30. The pit membrane of V–FT pit of an earlywood vessel after the sodium chlorite-acetic acid treatment. Microfibrils (arrowed) in the pit membrane are randomly dispersed.

Photo 31. V–R pits of an earlywood vessel as seen from the lumen side. The photo shows V–Ru pits with large elliptical shaped pit aperture at the upper and V–Rp pits with small slit-like pit aperture at the center. Ru: upright ray cell, Rp: procumbent ray cell.

Photo 32. V–Rp pits of an earlywood vessel as seen from the lumen side.

Photo 33. V–Rp pits of an earlywood vessel as seen from the outer surface wall.

Photo 34. A part of the photo 33 showing the detail of the V–Rp pits.

Photo 35. V–Rp pit of a latewood vessel as seen from the lumen side.

Photo 36. V–Rp pits of a latewood vessel as seen from the outer surface wall.

Photo 37. Split longitudinal radial surface of a vessel in the transitional zone from earlywood to latewood, after the sodium chlorite-acetic acid treatment. V–Rp pits as seen from the lumen side are shown at the upper in this photo. The direction of the major axis of slit-like pit apertures is almost parallel to the microfibrillar orientation in the S_2 layer. S_2: middle layer of secondary wall.

Photo 38. Inner surface wall of an earlywood vessel as seen from the lumen side. V-Rp pits are not found on the vessel wall being in contact with procumbent ray cells. Rp: procumbent ray cell.

Photo 39. V-Ru pits of an earlywood vessel as seen from the lumen side. Refer to photo 31.

Photo 40. V-Ru pits of a vessel in the transitional zone from earlywood to latewood as seen from the lumen side. The circular depressions (arrowed) in the pit membranes show the shape of the pit annulus of the upright ray cells in the opposite side.

Photo 41. V-Ru pits of a vessel in the transitional zone from earlywood to latewood as seen from the lumen side. These V-Ru pits are unilaterally compound pittings. The small circular depression (arrowed) in the pit membranes show the shape of the pit annulus of the upright ray cells in the opposite side.

Photo 42. A part of photo 41.

Photo 43. V-P pits (at the left) and V-FT pits (at the right) of an earlywood vessel as seen from the lumen side.

Photo 44. V-P pits of an earlywood vessel as seen from the lumen side.

Photo 45. V-P pits of an earlywood vessel as seen from the outer surface wall.

Photo 46. V-P pits (at the right) and V-FT pits (at the left) of a latewood vessel as seen from the lumen side.

Photo 47. V-P pits of a latewood vessel as seen from the lumen side.

Photo 48. V-P pits of a latewood vessel as seen from the outer surface wall.

Photo 49. Split longitudinal radial surface of an earlywood vessel wall, after the sodium chlorite-acetic acid treatment showing the microfibrillar orientation of the S_1, the S_{1-2}, the S_2, the S_{2-3} and the S_3 layers. S_1: outer layer of secondary wall, S_{1-2}: intermediate layer between the S_1 and the S_2 layers, S_2: middle layer of secondary wall, S_{2-3}: intermediate layer between the S_2 and the S_3 layers, S_3: inner layer of secondary wall.

Photo 50. A part of photo 49. S_1: outer layer of secondary wall, S_2: middle layer of secondary wall.

Photo 51. Split longitudinal radial surface of a latewood vessel wall, after the sodium chlorite-acetic acid treatment showing the warty layer and the microfibrillar orientation of the S_2 layer. WL: warty layer, S_2: middle layer of secondary wall.

Photo 52. Split longitudinal surface of a latewood vessel wall, after the sodium chlorite-acetic acid treatment showing the warty layer, the S_1 and the S_2 layers. WL: warty layer, S_1: outer layer of secondary wall, S_2: middle layer of secondary wall.

Photo 53. A part of photo 49. S_{1-2}: intermediate layer between the S_1 and the S_2 layers.

Photo 54. Split longitudinal radial surface of an earlywood vessel wall, showing the microfibrillar orientation of the S_2, the S_{2-3} and the S_3 layers. S_2: middle layer of secondary wall, S_{2-3}: intermediate layer between the S_2 and the S_3 layers, S_3: inner layer of secondary wall.

Photo 55. Split longitudinal radial surface of a latewood vessel wall, after the sodium chlorite-acetic acid treatment showing the warty layer, the microfibrillar orientation of the S_{2-3} and the S_2 layers. WL: warty layer, S_2: middle layer of secondray wall, S_{2-3}: intermediate layer between the S_2 and the S_3 layers.

Photo 56. A part of simple perforation of an earlywood vessel as seen from the lumen side. H: height of rim.

Photo 57. A part of simple perforation of an earlywood vessel as seen from the lumen side. The rim of the simple perforation is not bordered. Microfibrillar orientation of the S_3 layer is disturbed near the rim.

Photo 58. A part of the rim of simple perforation of an earlywood vessel as seen from the lumen side. The rim is not bordered. S: secondary wall, ML: compound middle lammella.

Photo 59. A part of simple perforation of an earlywood vessel as seen from the lumen side.

Photo 60. A part of photo 59. The rim is bordered.

Photo 61. A part of perforation plate with one bar of a latewood vessel. T: vessel element in this side, O: vessel element in the opposite side.

Photo 62. A part of photo 61. T: vessel element in this side, O: vessel element in the opposite side.

Photo 63. A part of scalariform perforation plate of a latewood vessel. Bars of the vessel element in this side can be barely found only near the rim (arrowed), but they disappear gradually from the margin toward the center of perforation plate.

Photo 64. A part of photo 63. Bars are bordered. B: border in rim.

Photo 65. Perforation plate with irregularly forked bars of a vessel in the late stage of the earlywood as seen from the lumen side.

Photo 66. A part of typical scalariform perforation plate of a latewood vessel as seen from the lumen side.

Photo 67. A part of scalariform perforation plate of a latewood vessel as seen from the outer surface wall. The microfibrillar orientation of the S_2 layer (arrowed) is almost parallel to bars. Bars are bordered.

Photo 68. Warts on the inner surface wall of scalariform perforation plate of a latewood vessel.

Photo 69. A part of multiple perforation plate of a latewood vessel. Bars in this side are forked irregularly.

Photo 70. A part of multiple perforation plate of a latewood vessel. Perforation plate of both vessel elements in this side and the opposite side does not form a regular pair.

Photo 71. A part of multiple perforation plate of a latewood vessel. Bars of the vessel elements in this side and the opposite side form a regular pair.

Photo 72. A part of multiple perforation plate of a latewood vessel. Bars of the vessel element in this side are forked irregularly, whereas perforation plate in the opposite side is foraminate.

Photo 73. A part of photo 72.

Photo 74. The combination of a scalariform perforation plate (in this side) and a foraminate perforation plate (in the opposite side) in a latewood vessel.

Photo 75. Do. The detail of the pores in the opposite side. Arrows indicate warts at the edge of aperture.

Photo 76. Lower end of a multiple perforation plate of a latewood vessel as seen from the lumen side.

Photo 77. Lateral margin of a multiple perforation plate of a latewood vessel. Membrane consisting of dispersed microfibrils remains in the lateral end of pore of perforation plate.

Photo 78. Multiple perforation plates of three vessels near the end of an annual ring.

Photo 79. A part of foraminate perforation plate of a vessel near the end of an annual ring.

Photo 80. Do. Warts of the vessel element in the opposite side can be found through the vessel cavity at the pores of the vessel element in this side.

Photo 81. Scalariform perforation plate of an earlywood tracheary element as seen from the outer surface wall.

Photo 82. A part of photo 81. Bars are bordered. Net-like membrane (arrows) are found in the lateral margin of the perforation plate.

Photo 83. A part of photo 81. Membranes remain in the lateral margin of the perforation plate.

Photo 84. A part of photo 81. A pit at the lower end of the scalariform perforation plate of an earlywood tracheary element as seen from the outer surface wall. Pit membrane is net-like structure consisting of the bundles of microfibrils. These microfibrils can be also found near the pit annulus (arrowed), so the microfibrils in the center of pit are continuous to the pit annulus although they can't be seen on the pit border in this photo.

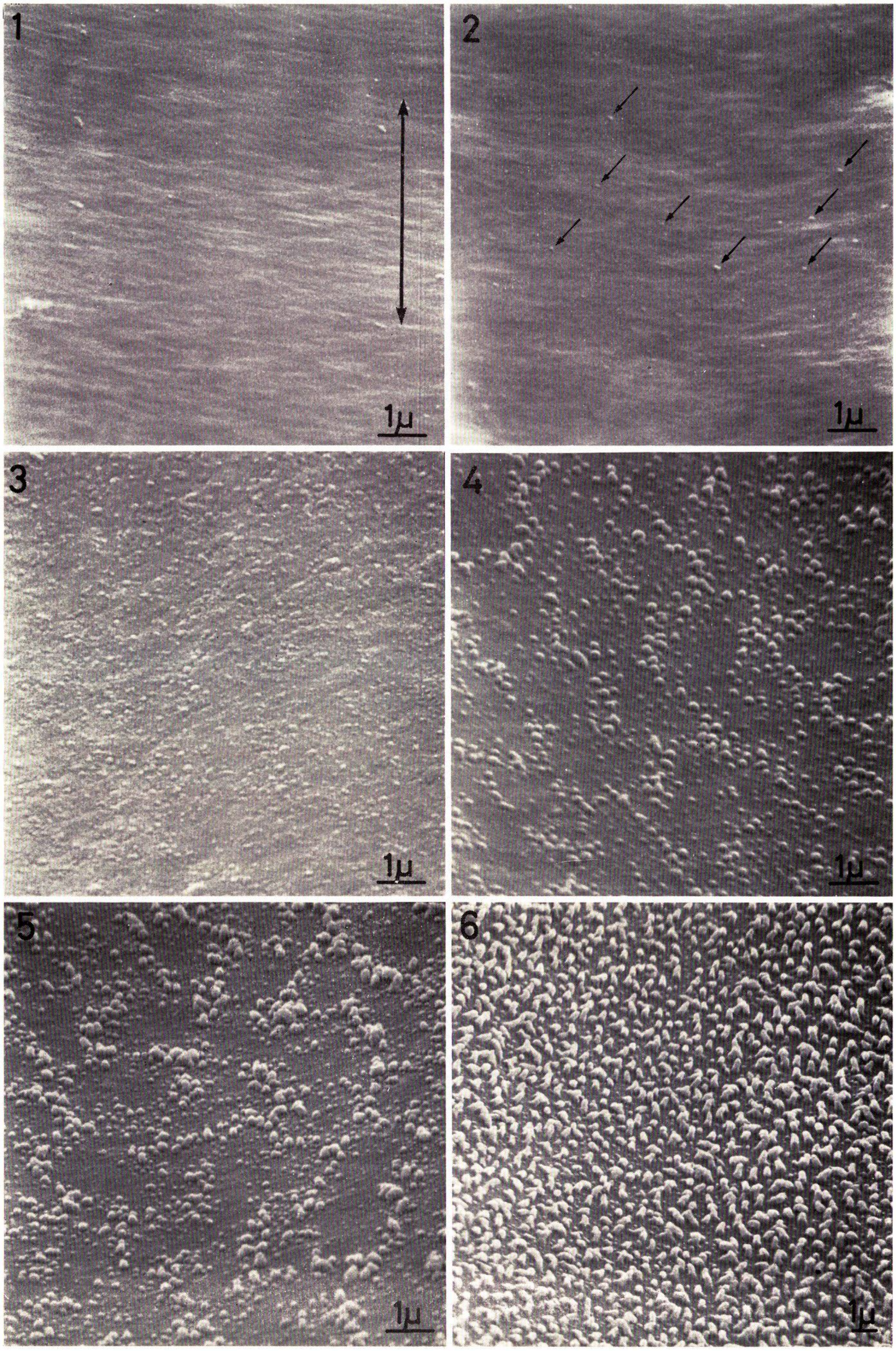
1
1μ
2
1μ
3
1μ
4
1μ
5
1μ
6
1μ

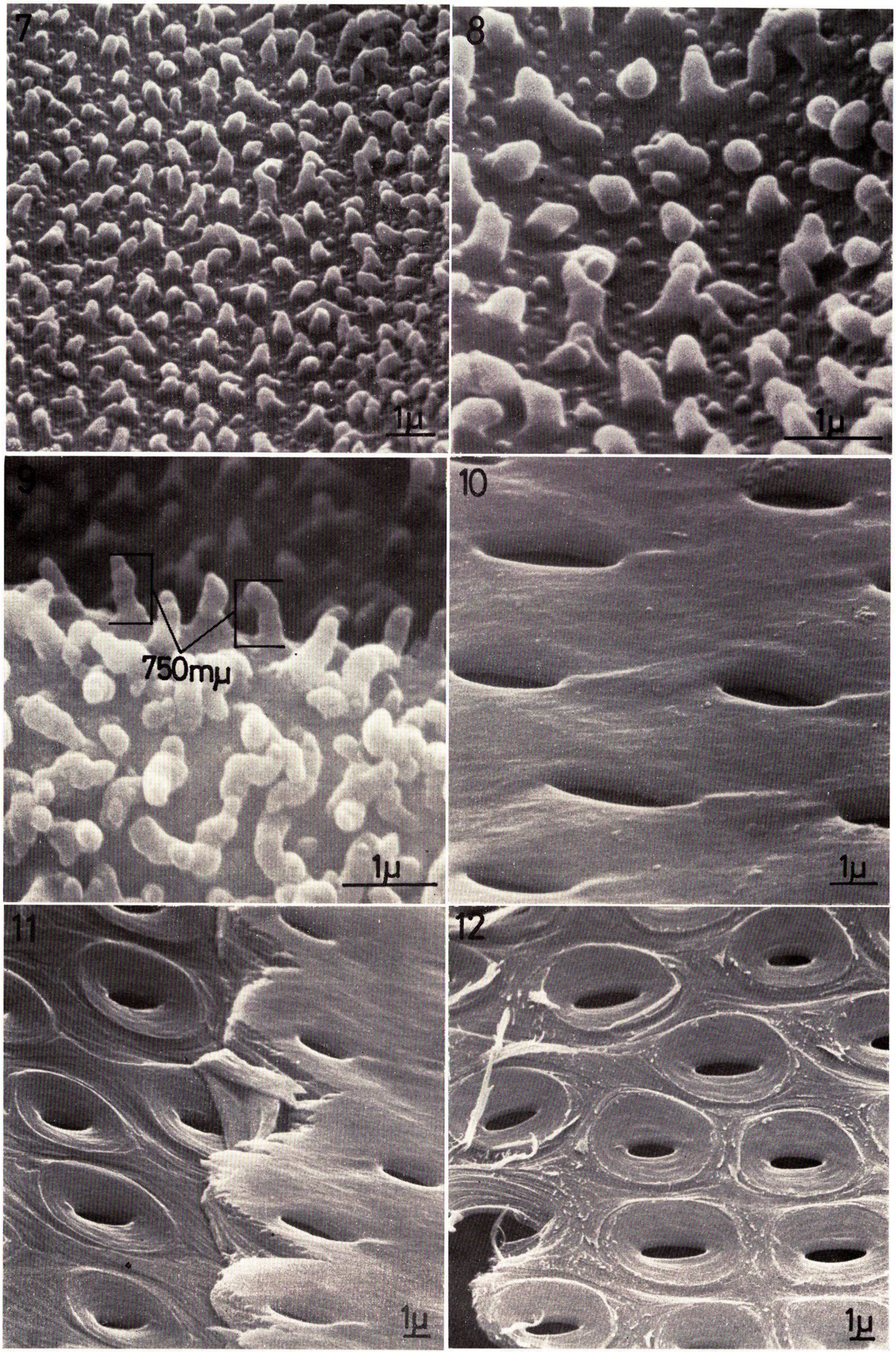
7
1μ
8
1μ
9
750mμ
1μ
10
1μ
11
1μ
12
1μ

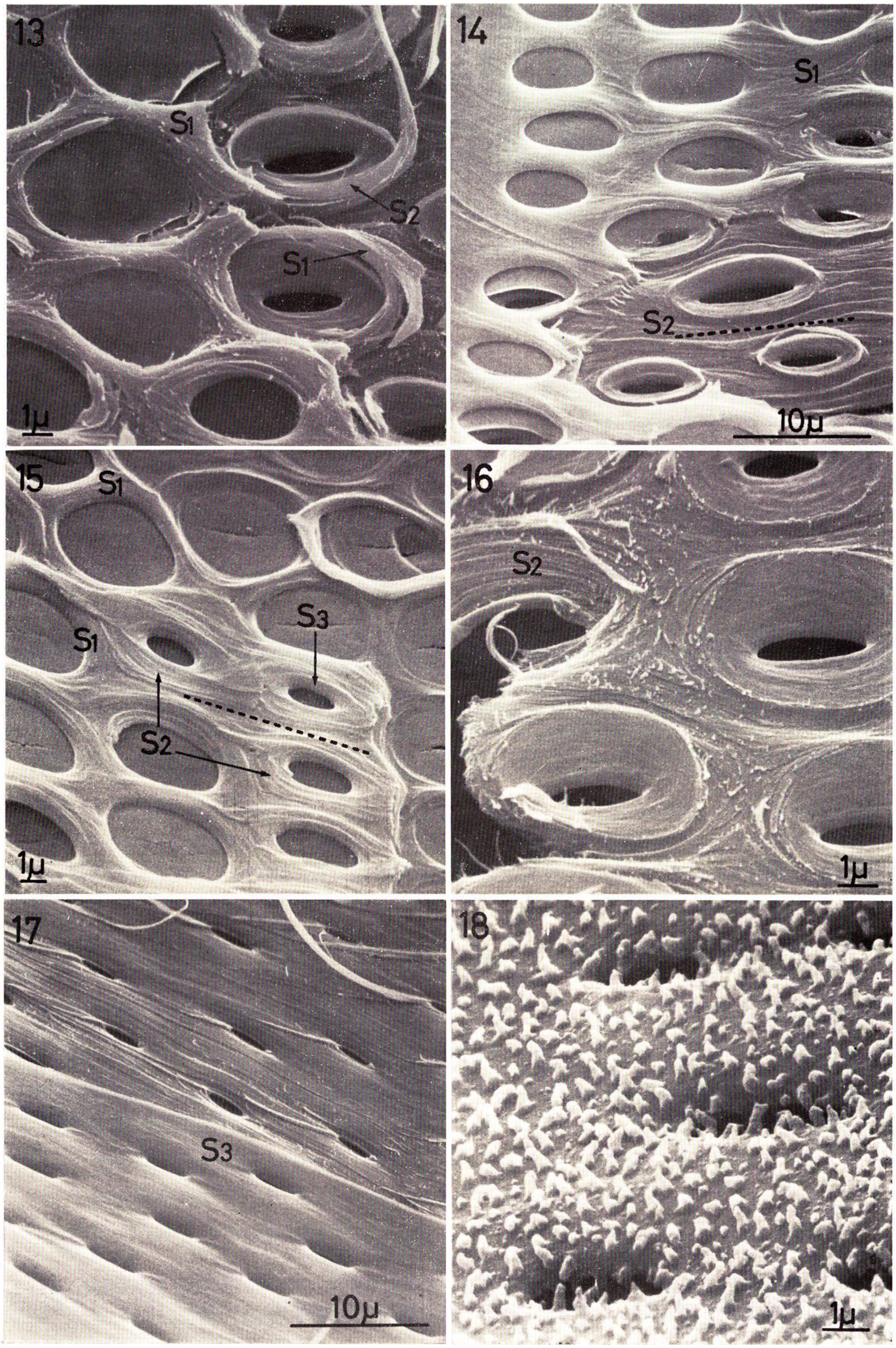
13
S1
S2
S1
1μ
14
S1
S2
10μ
15
S1
S1
S3
S2
1μ
16
S2
1μ
17
S3
10μ
18
1μ

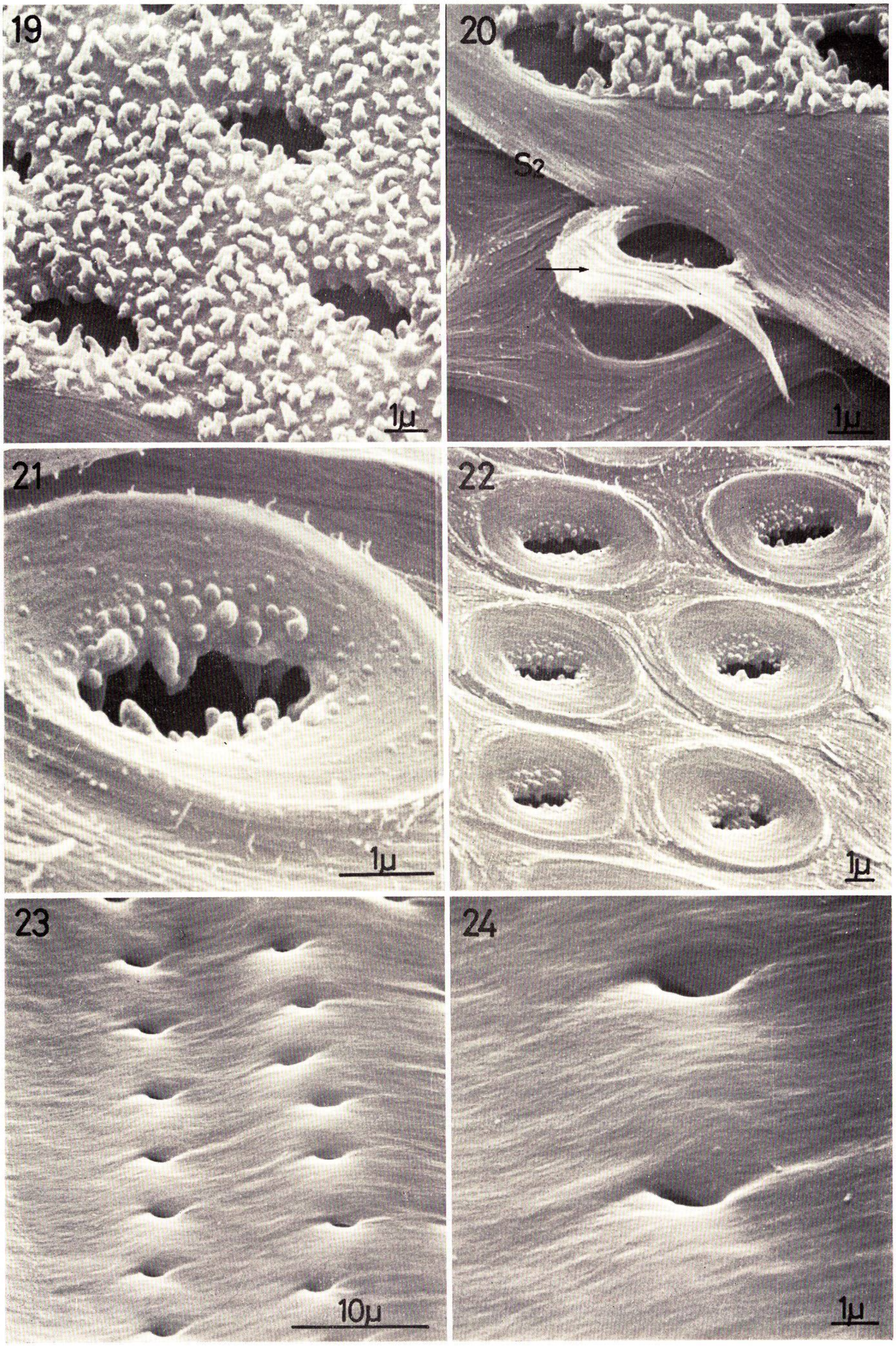
19
1μ
20
S2
1μ
21
1μ
22
1μ
23
10μ
24
1μ

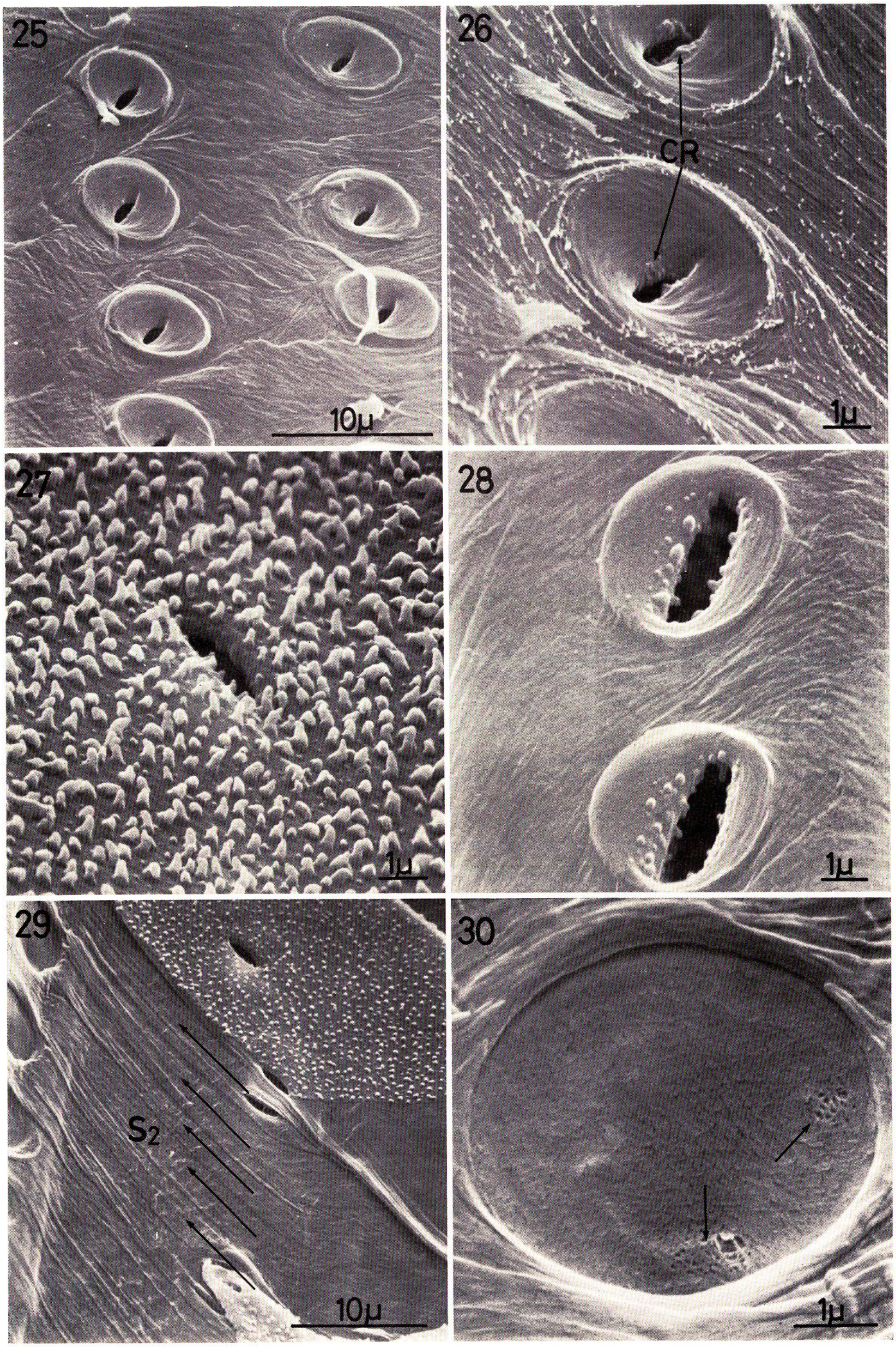
25
10μ
26
CR
1μ
27
1μ
28
1μ
29
S2
10μ
30
1μ

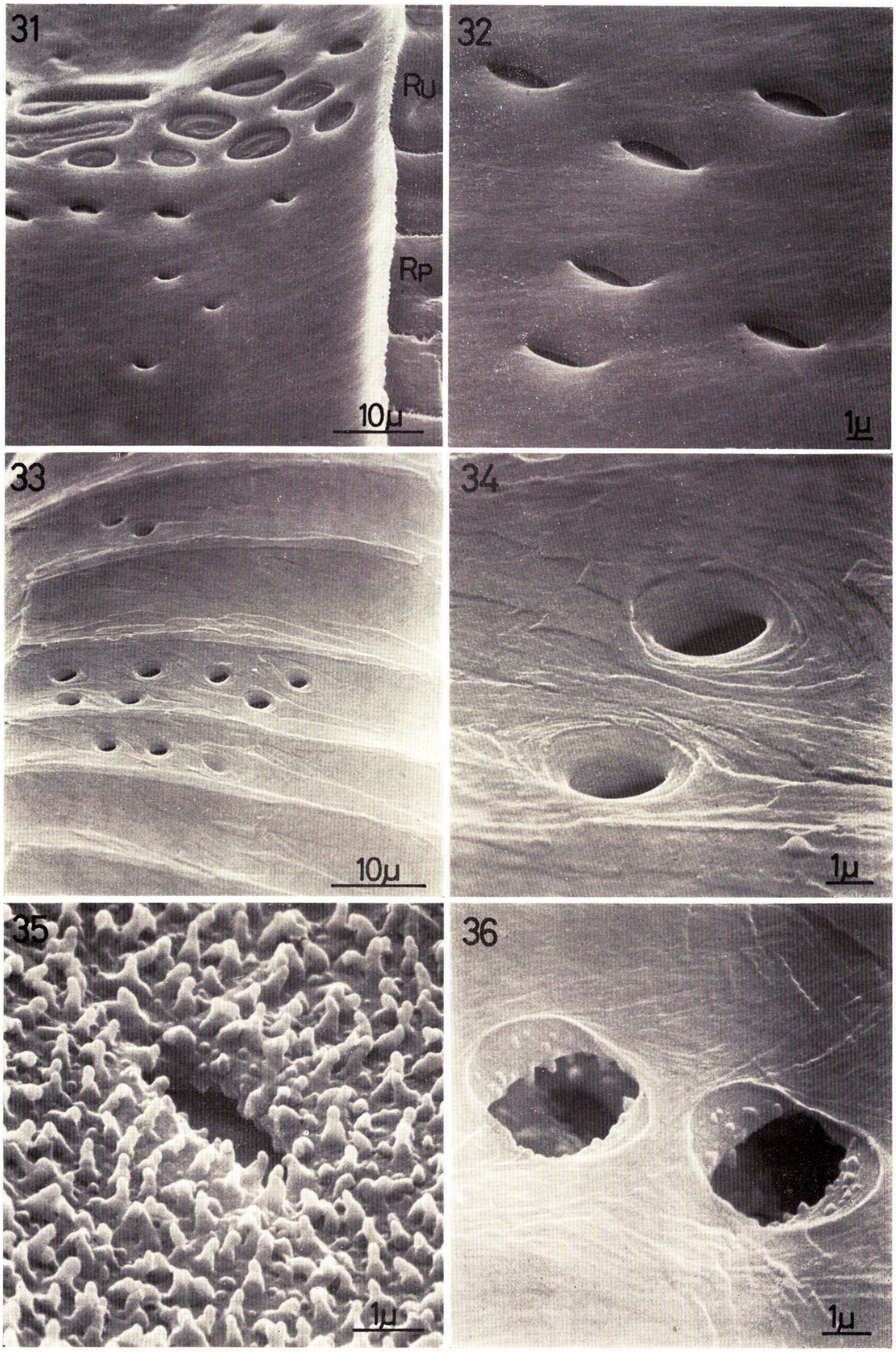
31
RU
RP
10μ
32
1μ
33
10μ
34
1μ
35
1μ
36
1μ

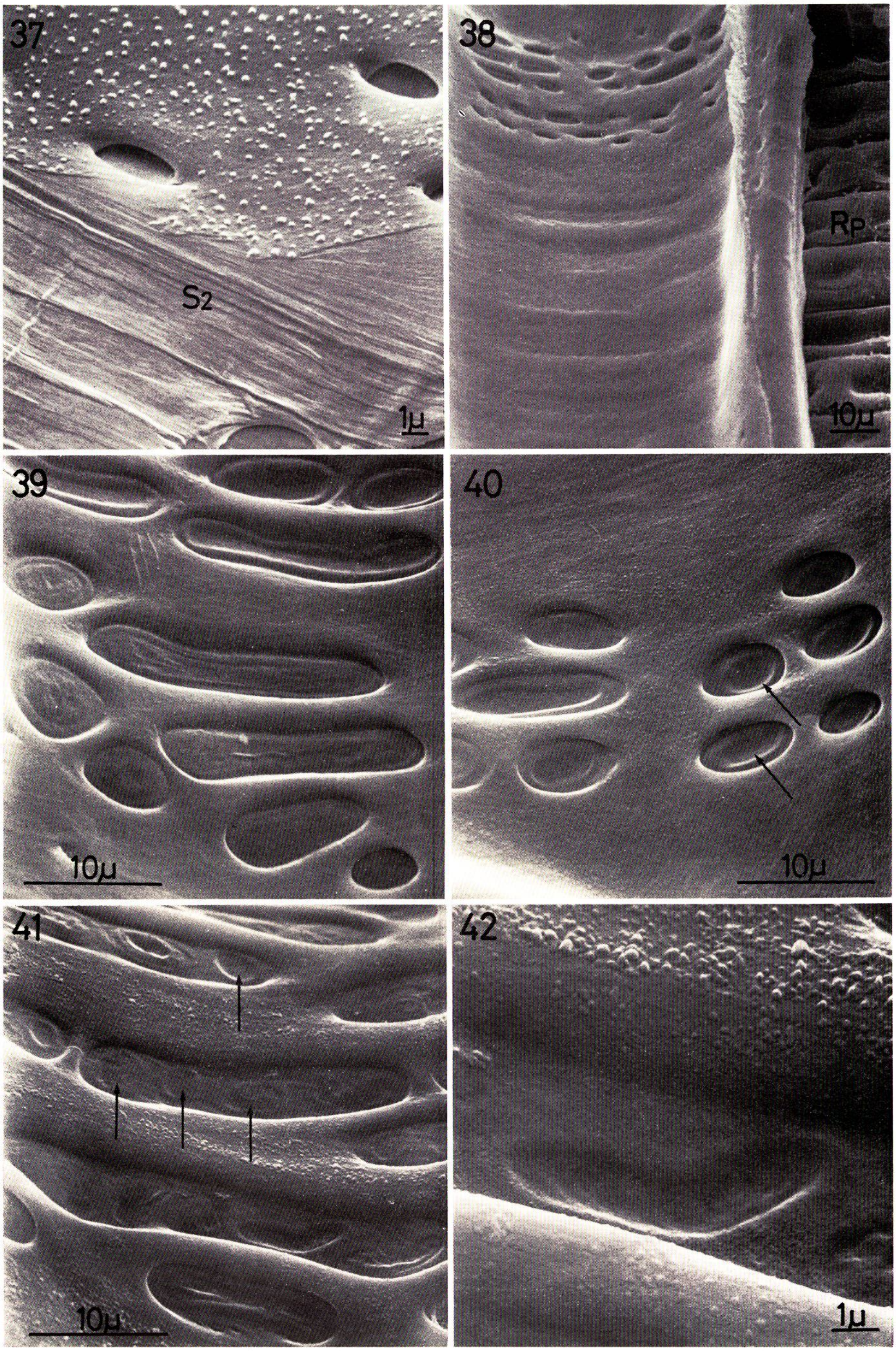
37
S2
1μ
38
RP
10μ
39
10μ
40
10μ
41
10μ
42
1μ

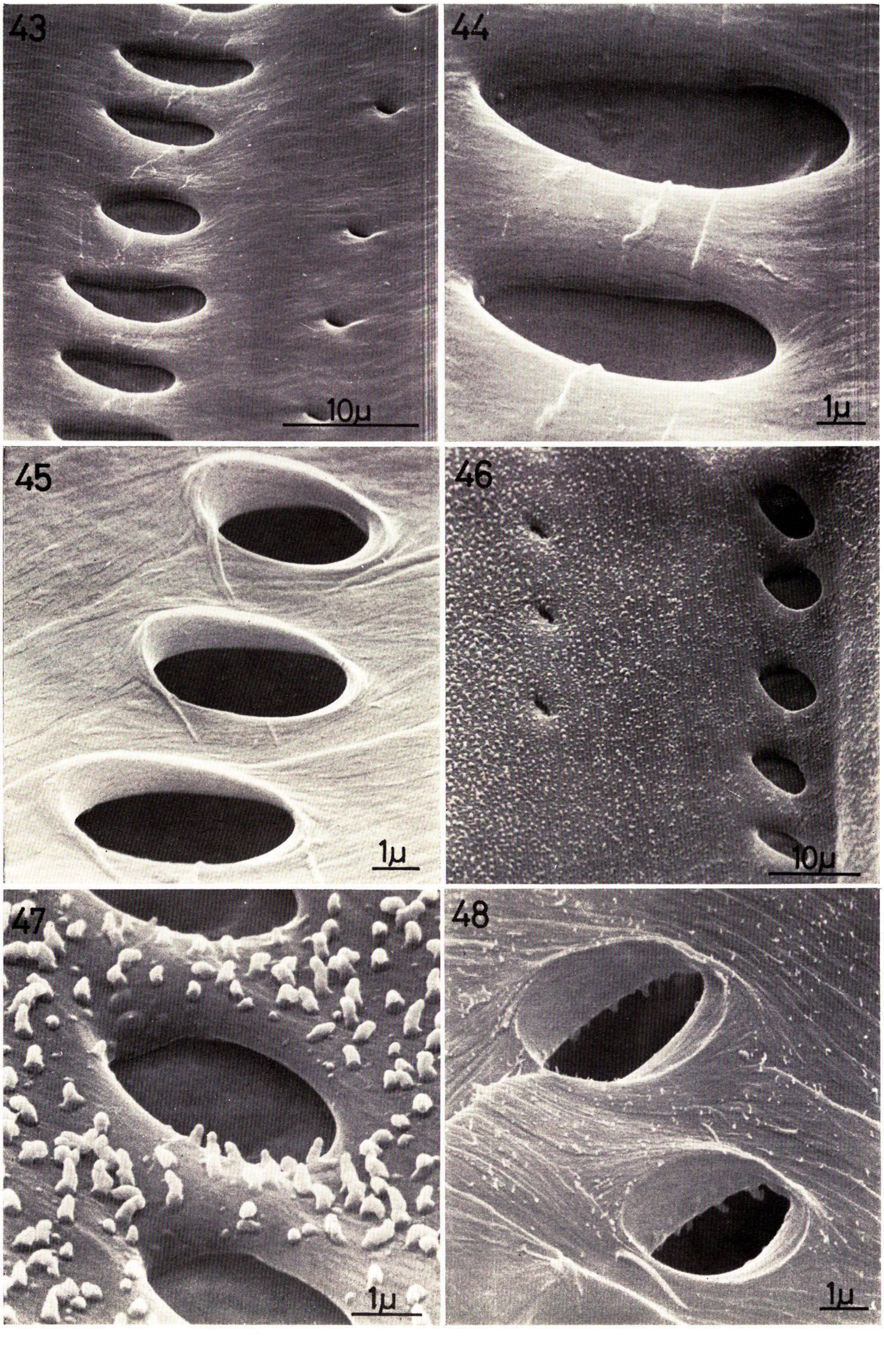
43
10μ
44
1μ
45
1μ
46
10μ
47
1μ
48
1μ

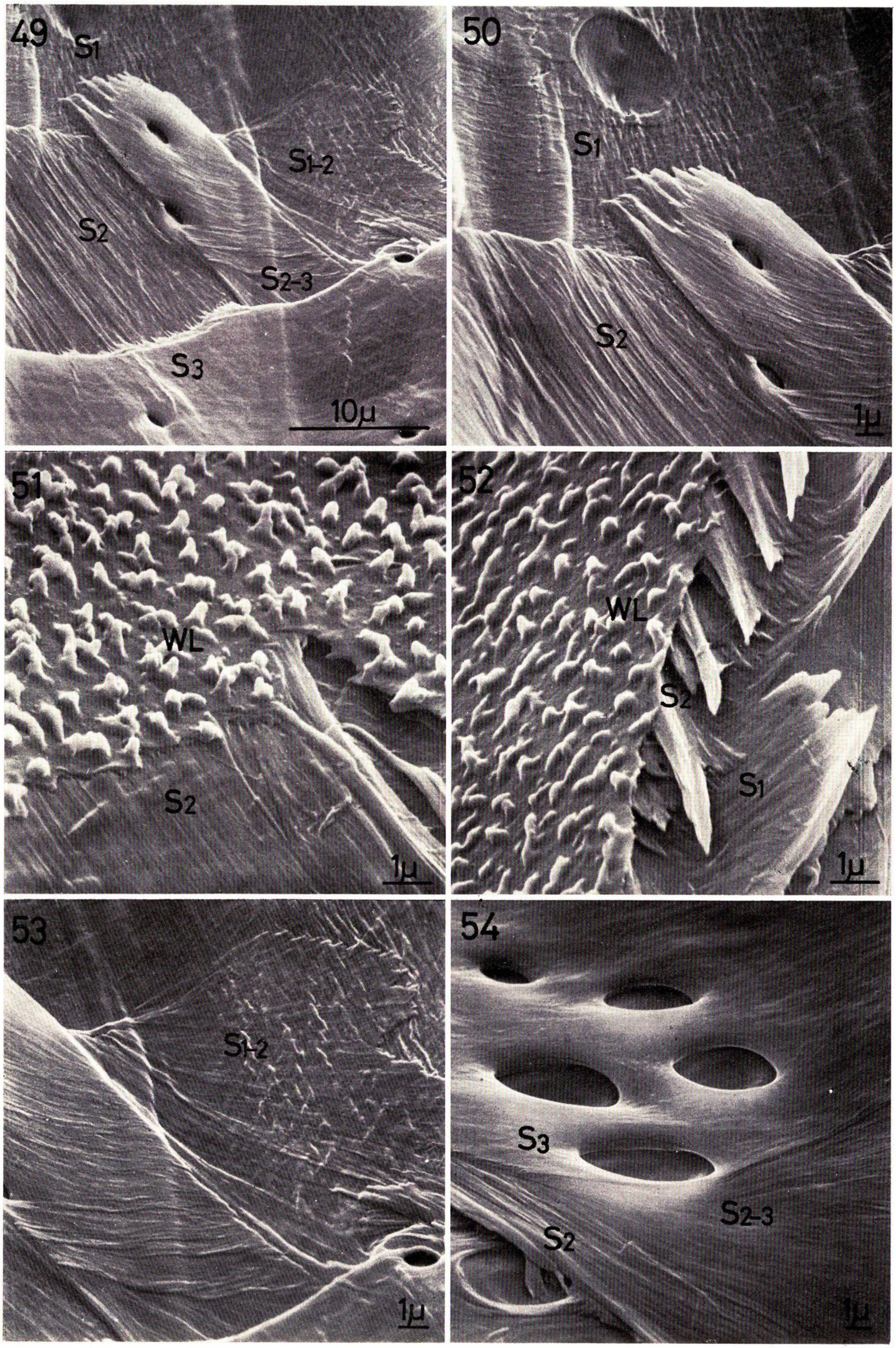
49
S_1
S_{1-2}
S_2
S_{2-3}
S_3
10μ
50
S_1
S_2
1μ
51
WL
S_2
1μ
52
WL
S_2
S_1
1μ
53
S_{1-2}
1μ
54
S_3
S_{2-3}
S_2
1μ

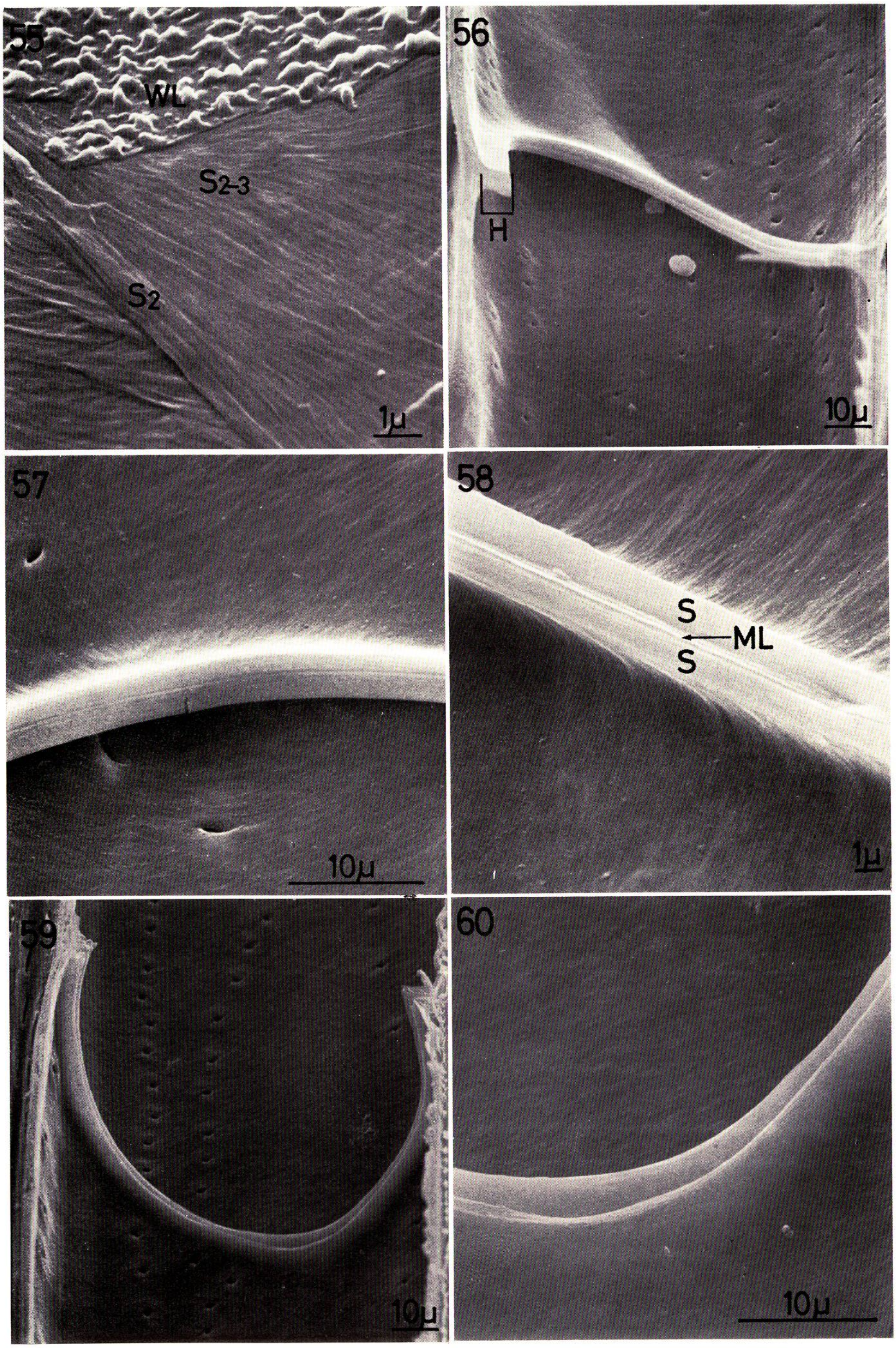
55
WL
S2-3
S2
1μ
56
H
10μ
57
10μ
58
S
ML
S
1μ
59
10μ
60
10μ

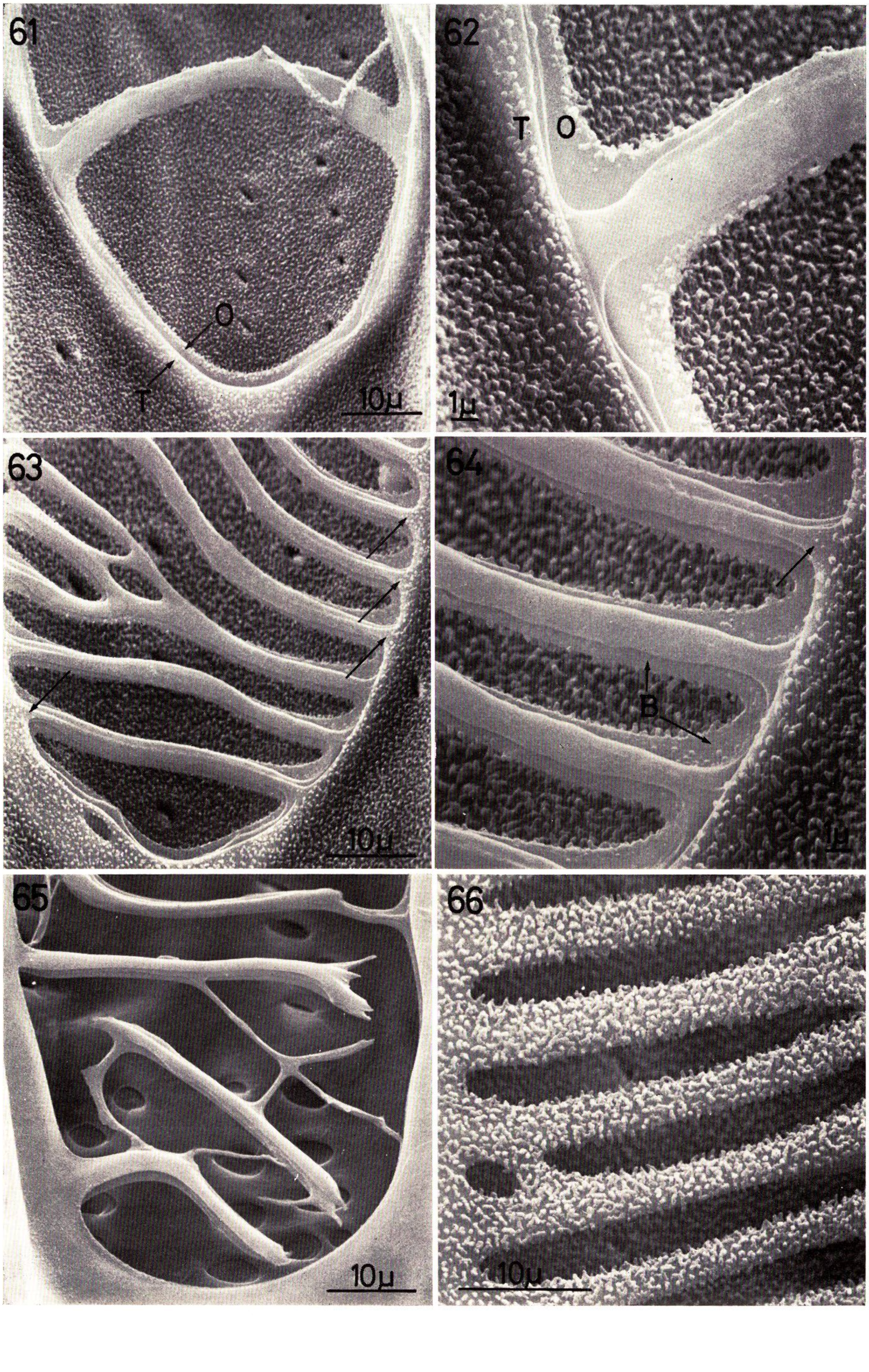
61
O
T
10μ
62
T O
1μ
63
10μ
64
B
1μ
65
10μ
66
10μ

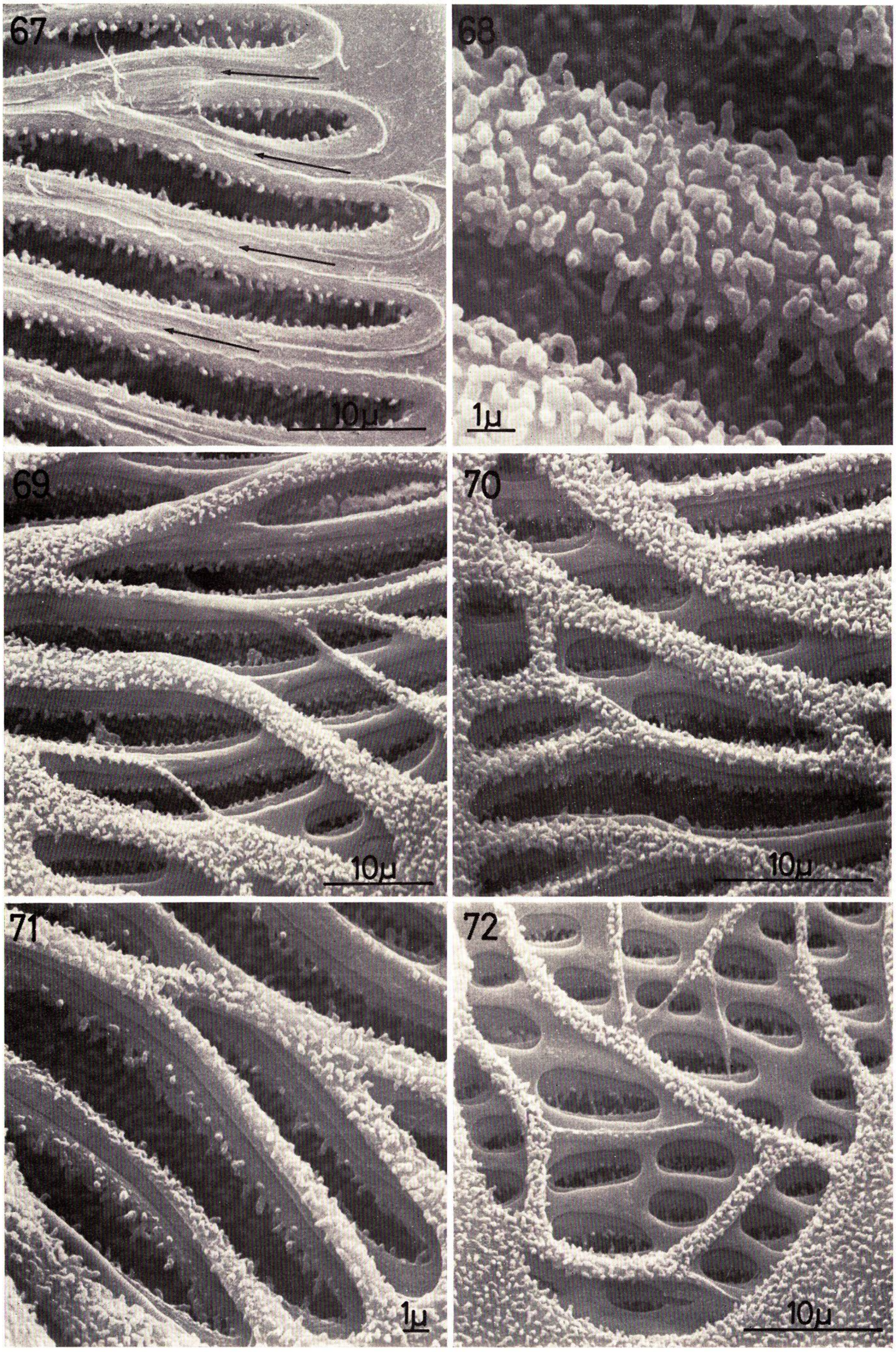
67
10μ
68
1μ
69
10μ
70
10μ
71
1μ
72
10μ

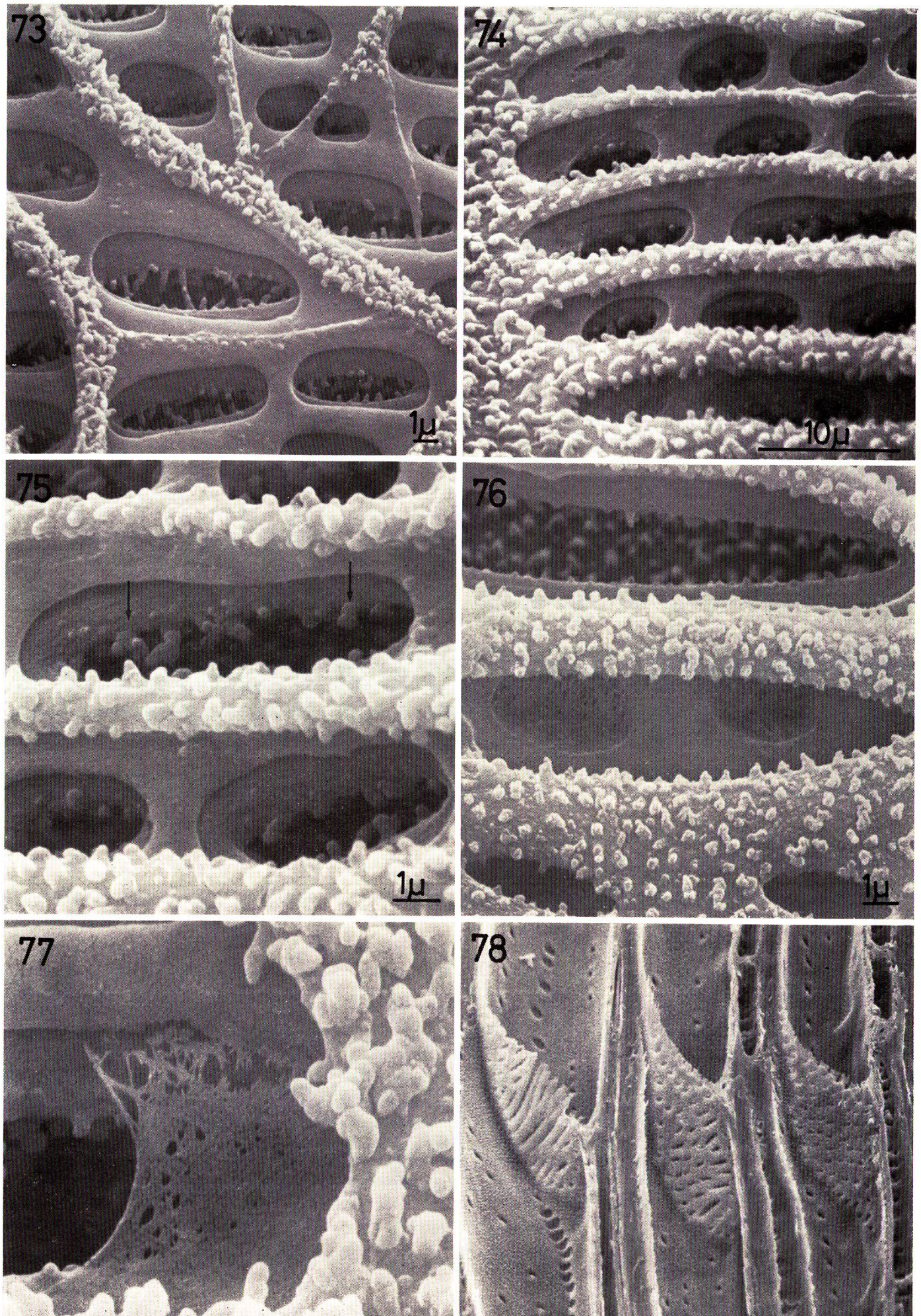
73
1μ
74
10μ
75
1μ
76
1μ
77
1μ
78
10μ

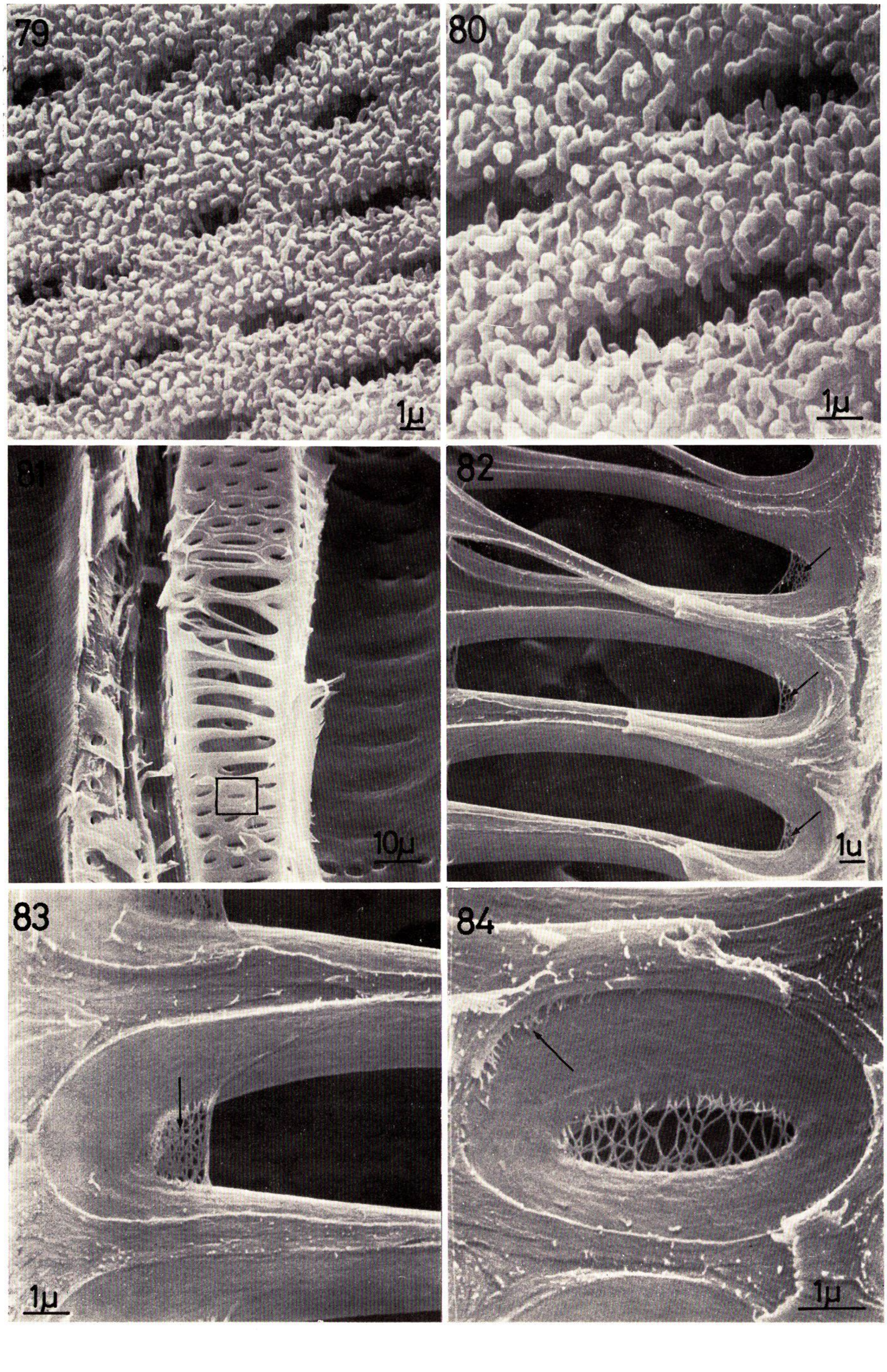
79
1μ
80
1μ
81
10μ
82
1u
83
1μ
84
1μ